Journal of Electroceramics, 13, 779–784, 2004

Defect Chemical Modeling of (La,Sr)(Co,Fe)$O_{3-\delta}$

EDITH BUCHER & WERNER SITTE*
Chair of Physical Chemistry, University of Leoben, A-8700 Leoben, Austria

Submitted February 11, 2003; Revised February 12, 2004; Accepted February 20, 2004

Abstract. Different defect chemical models for calculation of ionic and electronic defect concentrations are discussed regarding their applicability to transition metal perovskite-type oxides ($ABO_{3-\delta}$) with large ranges of oxygen non-stoichiometry. A point defect model, which allows simultaneous consideration of three different B-site species concentrations as a function of the oxygen partial pressure is compared to a simple point defect model, considering only two different B-site species. Additionally, a model assuming electrons/holes as negative resp. positive electronic charge carriers is presented. Further, models involving association of point defects in different complexes are discussed. Examples are given for fits of experimental data of $La_{1-x}Sr_xBO_{3-\delta}$ ($x = 0.6$, B = Fe, Co) to selected models in the temperature range 700–900°C and oxygen partial pressures $10^{-5} < pO_2/atm < 1$.

Keywords: perovskite-type oxides, oxygen non-stoichiometry, defect chemical modeling

Introduction

The perovskite-type oxides $La_{0.4}Sr_{0.6}CoO_{3-\delta}$ (LSC46) and $La_{0.4}Sr_{0.6}FeO_{3-\delta}$ (LSF46) are mixed conductors which exhibit high electronic and ionic conductivities. A variety of applications in electrochemical or catalytic devices, including cathodes of SOFCs, oxygen sensors, and semi-permeable membranes for conversion of methane to syn-gas, is conceivable.

Negative effective charges introduced by Sr-doping of $LaBO_{3-\delta}$ (B = Co, Fe) are compensated by formation of oxygen vacancies and/or electron holes. In the oxidizing pO_2-range these two mechanisms have oppositional effects. An increase of p-type charge carriers (B^{4+}-ions resp. electron holes) will enhance the electronic conductivity σ_e. Contrarily, formation of oxygen vacancies at the expense of the $B^{4+}/\dot{h}$-concentration increases the oxygen non-stoichiometry δ and therefore the ionic conductivity, while decreasing the electronic conductivity. Thus, knowledge of the dependence of the oxygen non-stoichiometry on temperature, oxygen partial pressure, and dopant degree is the basis for tailoring materials with specific transport properties.

*To whom all correspondence should be addressed. E-mail: sitte@unileoben.ac.at

Regarding transition metal perovskite-type oxides, (La,Sr)$FeO_{3-\delta}$ and especially (La,Sr)$CoO_{3-\delta}$ with high Sr-content exhibit particular features. Undoped $LaFeO_{3-\delta}$ and $LaCoO_{3-\delta}$, or compounds with low Sr-content ($x \leq 0.1$) show a rather 'ideal' behavior, e.g. dependences of $\delta \propto pO_2^{-1/2}$ in the high pO_2-region [1, 2]. However, deviations from the frequently observed dependence of δ vs. log pO_2 with three defined regions, as well as interaction of point defects can occur in compounds with high doping degree and significant concentrations of ionic and electronic defects. E.g., the absence of a plateau in the intermediate pO_2-range where $\delta \approx x/2$ independent of the oxygen partial pressure is typical for the solid solution $La_{1-x}Sr_xCoO_{3-\delta}$.

As a consequence, simple defect models often lead to unsatisfactory results. The objective of the present study is to provide a theoretical approach to the pO_2-dependence of the oxygen non-stoichiometry of highly doped LSC and LSF. A number of different models will be discussed and applied to experimental data.

Experimental

Samples of $La_{0.4}Sr_{0.6}CoO_{3-\delta}$ (LSC46) and $La_{0.4}Sr_{0.6}FeO_{3-\delta}$ (LSF46) were synthesized by

the glycine-nitrate method [3]. The oxygen non-stoichiometry δ of both compounds was measured as a function of temperature ($700 < T/^{\circ}\mathrm{C} < 900$) and oxygen partial pressure ($10^{-5} < p\mathrm{O}_2/\mathrm{atm} < 1$). Data for LSC46 were obtained by coulometric titrations in a closed electrochemical cell [4]. No hysteresis effects were observed between oxidation and reduction runs. The oxygen non-stoichiometry of LSF46 was determined by carrier gas coulometry (SensoTech, model Oxylyt) as well as thermogravimetry (TG) in a precision thermobalance (Setaram, model TAG 2416). Gas mixtures of Ar, Ar-O_2 (1 vol% O_2), and O_2 were adjusted by mass flow controllers (Tylan, model 2900). The oxygen partial pressure was measured by an oxygen sensor placed close to the sample in the thermobalance. Values of the absolute oxygen non-stoichiometry were obtained by total reduction in Ar-H_2 (1 vol% H_2) at 900°C.

Defect Chemical Models

The defect chemistry of transition metal perovskite-type oxides $La_{1-x}Sr_xBO_{3-\delta}$ with B = Fe, Co is described by two fundamental reactions. Using Kröger-Vink notation, the equilibrium between the solid oxide and the gas atmosphere is given by

$$\frac{1}{2}\mathrm{O}_2 + \mathrm{V}_\mathrm{o}^{\bullet\bullet} + 2\mathrm{B}_\mathrm{B}^x \Leftrightarrow \mathrm{O}_\mathrm{o}^x + 2\mathrm{B}_\mathrm{B}^\bullet. \tag{1}$$

The corresponding equilibrium constant determining the release and uptake of oxygen can be obtained from the mass action law

$$K_\mathrm{ox} = \frac{\left[\mathrm{O}_\mathrm{o}^x\right]\left[\mathrm{B}_\mathrm{B}^\bullet\right]^2}{\mathrm{pO}_2^{1/2}[\mathrm{V}_\mathrm{o}^{\bullet\bullet}]\left[\mathrm{B}_\mathrm{B}^x\right]^2}. \tag{2}$$

Further, charge disproportionation of the B-site ion, expressed by the reaction

$$2\mathrm{B}_\mathrm{B}^x \Leftrightarrow \mathrm{B}_\mathrm{B}' + \mathrm{B}_\mathrm{B}^\bullet, \tag{3}$$

with the equilibrium constant

$$K_i = \frac{\left[\mathrm{B}_\mathrm{B}'\right]\left[\mathrm{B}_\mathrm{B}^\bullet\right]}{\left[\mathrm{B}_\mathrm{B}^x\right]^2}, \tag{4}$$

describes the redistribution of electronic charges. In this point defect model electrons and electron holes are assumed to be localized on specific B-site ions. Three additional expressions are obtained from the electroneutrality condition, Eq. (5), and the site conservation requirements for O-site respectively B-site species, Eqs. (6) and (7)

$$[\mathrm{Sr}_\mathrm{La}'] + [\mathrm{B}_\mathrm{B}'] = \left[\mathrm{B}_\mathrm{B}^\bullet\right] + 2\left[V_o^{\bullet\bullet}\right], \tag{5}$$

$$[\mathrm{V}_\mathrm{o}^{\bullet\bullet}] + \left[\mathrm{O}_\mathrm{o}^x\right] = 3, \tag{6}$$

$$\left[\mathrm{B}_\mathrm{B}^x\right] + [\mathrm{B}_\mathrm{B}'] + [\mathrm{B}_\mathrm{B}^\bullet] = 1. \tag{7}$$

The Sr-content and the oxygen vacancy concentration are given by $[\mathrm{Sr}_\mathrm{La}'] = x$ and $[V_O^{\bullet\bullet}] = \delta$, respectively. Therefore, a set of five equations is obtained, Eqs. (2) and (4)–(7), which can be solved analytically for an expression $\mathrm{pO}_2 = f(K_i, K_\mathrm{ox}, x, \delta)$. Parameters K_i and K_{ox} are determined by nonlinear least squares fits. At intermediate oxygen partial pressures the point defect model predicts a plateau in the log pO_2-dependence of the oxygen non-stoichiometry at $\delta \approx x/2$. However, with decreasing ratio K_ox/K_i the plateau diminishes and can even disappear (compare e.g. oxygen non-stoichiometry of LSC46 in Fig. 1). Due to the B-site conservation condition (Eq. (7)) the theoretical maximum oxygen non-stoichiometry predicted by the point defect model at low pO_2 is $\delta_\mathrm{max} = 0.5 + x/2$.

For the high pO_2-range (approx. 10^{-5}-1 atm) a simplified version of the point defect model neglecting the

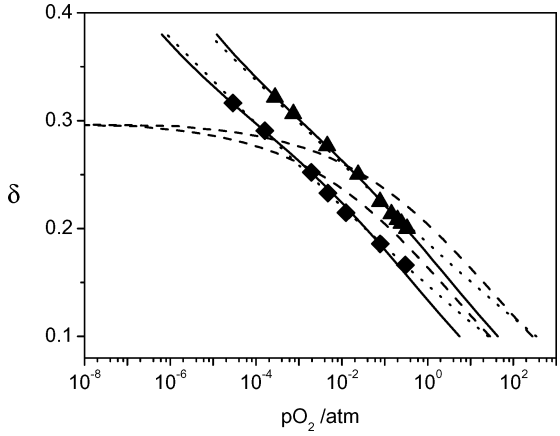

Fig. 1. Experimental data of the oxygen non-stoichiometry of $La_{0.4}Sr_{0.6}CoO_{3-\delta}$ at 750° (♦) and 825°C (▲). Lines are nonlinear least squares fits to the point defect model (solid), the simple point defect model (dashed), and the itinerant electron model (Refs. [5, 6], dotted).

concentration of divalent B-site ions can be applied, provided that $[B_B^{\bullet}] \gg [B'_B]$. However, this simple point defect model is limited to oxygen non-stoichiometry values $\delta < x/2$ and cannot describe the transition from p- to n-type regime occurring at lower pO_2. Nevertheless, the applicability of this simplification to our experimental data is evaluated in the present study. Supposing that $[B'_B] \rightarrow 0$ Eqs. (5) and (7) can be simplified. Combination with Eqs. (2) and (6) results in a set of four equations which can be solved analytically for $pO_2 = f(K'_{ox}, x, \delta)$ with a single fit parameter K'_{ox}. Within the point defect models given above, electronic charge carriers are assigned to specific B-site ions (B^{2+} resp. B^{4+}). The following model works with electronic charge carriers of the form e' and $h^{\cdot}$. Alternatively to a redox reaction with different oxidation states of B-site ions (see Eq. (1)), an approach based on the oxygen ion balance with creation respectively consumption of electronic charge carriers can be applied

$$\frac{1}{2}O_2 + V_0^{\bullet\bullet} + 2e' \Leftrightarrow O_o^x. \tag{8}$$

Considering the equilibrium for annihilation/formation of electronic charge carriers

$$0 \Leftrightarrow e' + h^{\bullet}, \tag{9}$$

and the electroneutrality condition given by

$$\left[Sr'_{La}\right] + \left[e'\right] = 2\left[V_o^{\bullet\bullet}\right] + \left[h^{\bullet}\right], \tag{10}$$

the equilibrium constants K''_{ox} and K_e for Eqs. (8) and (9) can be derived as mass action law expressions analogous to Eqs. (2) and (4). In contrast to the point defect model where, due to B-site conservation requirements, the concentration of B'_B (n-type charge carriers) and therefore the oxygen vacancy concentration at low pO_2 are limited, the electronic charge carrier model does not imply a comparable limitation of $[e']_{max}$. Theoretically, a maximum oxygen non-stochiometry $\delta_{max} = 3$ could be obtained from the electronic charge carrier model at sufficiently low pO_2. Of course this maximum cannot be reached in practice due to the decomposition of the perovskite phase.

Further, the itinerant electron model suggested by Lankhorst et al. [5, 6] for the oxygen non-stoichiometry of $La_{1-x}Sr_xCoO_{3-\delta}$, which predicts an almost linear dependence of δ on log pO_2 (theoretically up to $\delta_{max} = 3$) was applied to our experimental data of LSC46. The semi-empirical approach proposed by Yang et al. [7] which is based on a point defect model with empirical assumptions was also used for fits to data of LSC46 and LSF46.

In principle, the dilute solution approach of independent point defects is only valid in the near-stoichiometric region where defect concentrations are small (< 0.1%). For systems with high values of oxygen non-stoichiometry, like LSC46 and LSF46, formation of defect associates is conceivable and new highly ordered phases can be formed with increasing defect concentration. A number of models involving defect complexes have been proposed for $La_{1-x}Sr_xBO_{3-\delta}$ (B = transition metal). Formation of associated defects could occur via charge interaction of (i) $V_O^{\bullet\bullet}$ and Sr'_{La}, or (ii) $V_O^{\bullet\bullet}$ and B'_B. Type (i) pair clusters $\{Sr'_{La} - V_O^{\bullet\bullet}\}^{\bullet}$ were reported to be energetically unfavorable for compounds with B = Fe, Cr, Mn in molecular dynamic studies [8, 9]. An exception is Sr-doped $LaCoO_3$ where calculations confirmed a tendency towards formation of type (i) clusters. Models based on type (ii) complexes $\{B'_B - V_O^{\bullet\bullet} - B'_B\}^x$ were suggested for undoped $LaBO_{3-\delta}$ CB = Mn, Co, Fe) by van Roosmalen et al. [10] as well as for $SrFeO_{3-\delta}$ by Kozhevnikov et al. [11] and Diethelm et al. [12]. Gavrilova et al. [13] proposed a similar model assuming that only a certain fraction of oxygen vacancies is associated in $\{B'_B - V_O^{\bullet\bullet}\}^{\bullet}$ clusters.

Analytical solutions of $pO_2 = f(\delta)$ as obtained for all models in this section are used for fits to our experimental data of the oxygen non-stoichiometry. Fit parameters are determined by iterative minimization of the sum of squared residuals $\sum_{i=1}^{n} (\log pO_{2,\,mod} - \log pO_{2,exp})^2$ by the Levenberg-Marquardt method, where $pO_{2,exp}$ represents the experimentally determined oxygen partial pressure and $pO_{2,mod}$ the value predicted by the respective defect chemical model at a defined value of oxygen non-stoichiometry δ_{exp}. Calculations are performed using the computer program *Mathematica* (Wolfram Research). Careful selection of the starting values for the iterative optimization is crucial as local minima can lead to physically impossible solutions (e.g. negative values of equilibrium constants). 2D- resp. 3D-plots of the sum of squared residuals as a function of the fit parameter(s) are helpful to estimate reasonable starting values. With the convergence tolerance <0.001 for the relative change of the sum of squared residuals between two successive iterations, convergence was usually reached in less than 10 iterative steps.

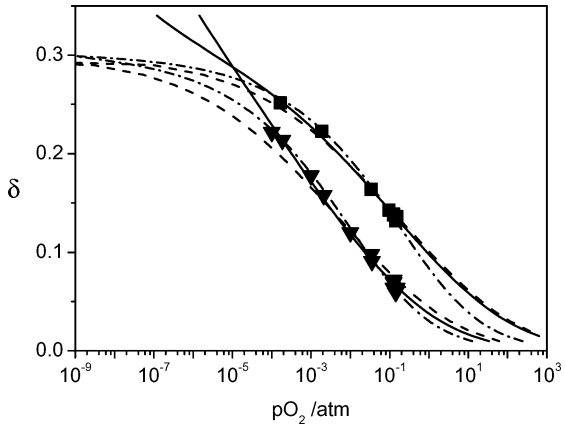

Fig. 2. Experimental data of the oxygen non-stoichiometry of $La_{0.4}Sr_{0.6}FeO_{3-\delta}$ at 700° (▼) and 900°C (■). Lines are nonlinear least squares fits to the point defect model (solid), the simple point defect model (dashed), and the electronic charge carrier model (dash-dotted).

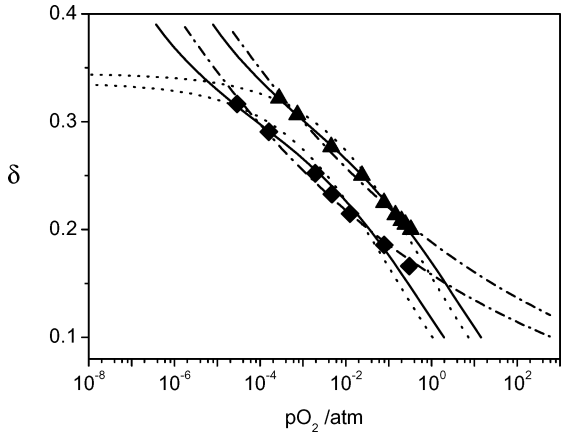

Fig. 3. Experimental data of the oxygen non-stoichiometry of $La_{0.4}Sr_{0.6}CoO_{3-\delta}$ at 750° (◆) and 825°C (▲). Lines are nonlinear least squares fits to the electronic charge carrier model (solid), the semi-empirical model (Ref. [7], dash-dotted), and the $\{B'_B - V_O^{\bullet\bullet}\}^{\bullet}$ cluster model (Ref. [13], dotted).

Results and Discussion

Experimental data of LSC46 obtained from coulometric titrations at temperatures 680°–825°C show an almost linear dependence of oxygen non-stoichiometry on log pO_2 even for $\delta > 0.3$, as seen in Fig. 1 for 750° and 825°C. This behavior as well as the magnitude of oxygen non-stoichiometry is consistent with other studies on $La_{1-x}Sr_xCoO_{3-\delta}$ with comparable Sr-content [1, 5]. Oxygen non-stoichiometry data of LSF46 (Fig. 2) determined from temperature runs (thermogravimetry as well as carrier gas coulometry) are in good agreement with those obtained from pO_2-runs (TG). The experimental error of oxygen non-stoichiometry measurements is estimated as ±2% (i.e. approximately the size of symbols in Figs. 1–3).

Fits of different defect chemical models to experimental data of LSC46 and LSF46 are given in Figs. 1–3. For the point defect model, the simple point defect model, and the electronic charge carrier model the respective fit parameters are summarized in Table 1.

In the pO_2-range 10^{-5} – 1 atm the point defect model taking into account three different valence states of the B-site ion is a good approximation for data of LSC46, see Fig. 1. Relatively low ratios of the equilibrium constants K_{ox}/K_i (Table 1) are found which describe the almost linear dependence of δ on log pO_2 at 750° and 825°C. Even though fits of the point defect model to the data of LSF46 yield coefficients of determination

Table 1. Equilibrium constants obtained from different defect chemical models for $La_{0.4}Sr_{0.6}CoO_{3-\delta}$(LSC46) and $La_{0.4}Sr_{0.6}FeO_{3-\delta}$(LSF46). Equilibrium constants refer to $pO_2^0 = 1$ atm.

	LSC46		LSF46	
	750°C	825°C	700°C	900°C
point defect model				
K_{ox}	5.8 ± 0.4	2.11 ± 0.05	$(1.10 \pm 0.04) \times 10^2$	$(1.40 \pm 0.04) \times 10^1$
K_i	$(5.9 \pm 0.7) \times 10^{-3}$	$(7.7 \pm 0.2) \times 10^{-3}$	$(3.1 \pm 0.3) \times 10^{-2}$	$(2.9 \pm 0.6) \times 10^{-3}$
simple point defect model				
K'_{ox}	2 ± 1	$(8 \pm 3) \times 10^{-1}$	$(7.3 \pm 0.7) \times 10^1$	$(1.26 \pm 0.06) \times 10^1$
electronic charge carrier model				
K''_{ox}	$(2.8 \pm 0.9) \times 10^5$	$(5.8 \pm 0.3) \times 10^4$	$(5.1 \pm 0.1) \times 10^9$	$(3.4 \pm 0.1) \times 10^{10}$
K_e	$(3.5 \pm 0.7) \times 10^{-3}$	$(4.7 \pm 0.2) \times 10^{-3}$	$(7.5 \pm 0.1) \times 10^{-5}$	$(1.40 \pm 0.02) \times 10^{-5}$

R^2 close to unity, extrapolations of fit functions towards lower pO_2 are not reasonable. Regarding LSF46 the point defect model predicts an intersection of fit functions at pO_2=10^{-5}atm (Fig. 2) which is most likely an artifact due to lack of data points at $pO_2 < 10^{-4}$ atm, resulting in fit parameters K_i which are overestimated with respect to K_{ox} at 700° and 900°C. This leads to a steep increase of δ with decreasing pO_2 whereas measurements of the oxygen non-stoichiometry of LSF46 in the intermediate pO_2-range (10^{-9}–10^{-11} atm) exhibit a plateau region in vicinity of $\delta = 0.3$, which implicates higher ratios of K_{ox}/K_i [2].

In case of LSF46, the electronic charge carrier model as well as the simple point defect model provide more reasonable extrapolations of oxygen non-stoichiometry towards lower pO_2, approaching $\delta = x/2 = 0.3$ with a decrease in slope, see Fig. 2. The simplified point defect model which neglects the concentration of divalent B-site ions can be used as an approximation for the ferrite LSF46 (Fig. 2). However, in case of the cobaltite LSC46 (Fig. 1) significant deviations of the simple point defect model from the experimental data occur and fit parameters exhibit large standard errors (Table 1). This can be interpreted by differences in the B^{2+}-concentrations in the pO_2-range under investigation. Using equilibrium constants obtained from the point defect model for calculation of $[B^{2+}]$, $[B^{3+}]$, and $[B^{4+}]$ as a function of pO_2, an increase of $[Co^{2+}]$ in LSC46 at $pO_2 < 10^{-2}$ atm is predicted, while $[Fe^{2+}]$ in LSF46 seems negligible over the pO_2-range 10^{-5}–1 atm.

The model assuming electronic charge carriers e' and $h^{\cdot}$ is a good approximation for experimental data of both LSC46 and LSF46 (Figs. 2 and 3, Table 1). Extrapolations towards lower pO_2 predict a progressive increase of δ with decreasing pO_2 in case of LSC46 and approach a plateau at $\delta = 0.3$ in case of LSF46.

For comparison fit functions obtained from the itinerant electron model are given for LSC46 in Fig. 1. This model implies an almost linear dependence of δ on log pO_2 and is therefore a good approximation for our experimental data of LSC46. Fit parameters obtained from the itinerant electron model are in agreement with literature results for similar compositions of $La_{1-x}Sr_xCoO_{3-\delta}$ [5, 6].

The semi-empirical model derived by Yang et al. [7] for the high pO_2-range is based on the assumption that $[B_B^{\bullet}]^2/[B_B^x]^2$ vs. pO_2 follows a power law. The validity of this relation was checked for our data sets preliminary to each fit, with $[B_B^{\bullet}]$ and $[B_B^x]$ calculated from the point defect model. Reasonable agreement was obtained for oxygen non-stoichiometry data of LSC46 (see Fig. 3) and LSF46 in the temperature range 700°–900°C at $10^{-5} < pO_2/\text{atm} < 1$. However, besides the empirical relation involved, a drawback of this model is the neglect of n-type electronic charge carriers, which should become of increasing importance with decreasing pO_2.

The $\{B'_B - V_O^{\bullet\bullet} - B'_B\}^x$ defect cluster model suggested for $LaBO_3$ (B = Mn, Fe, Co) by van Roosmalen et al. [10] was not suitable for the compounds under investigation which exhibit significant concentrations of p-type charge carriers in the oxidizing pO_2-range. For $SrFeO_{3-\delta}$, the applicability of this model was also reported to be restricted to the highest pO_2-region ($pO_2 > 10^{-2}$ atm at 900°C) [12]. Van Roosmalen et al. [10] provided an adaptation involving $\{B_B^x - V_O^{\bullet\bullet} - B_B^x\}^{\bullet\bullet}$ clusters for systems with significant divalent dopant concentration, which resembles the simple point defect model neglecting the concentration of B'_B (see above). Therefore, it is not surprising that the $\{B_B^x - V_O^{\bullet\bullet} - B_B^x\}^{\bullet\bullet}$ cluster model provides a satisfactory approximation for data of LSF46 at 700° and 900°C but not for data of LSC46.

The approach involving $\{B'_B - V_O^{\bullet\bullet}\}^{\bullet}$ complex formation by Gavrilova et al. [13] was derived under the assumption that the fraction of associated oxygen vacancies is independent of pO_2, implicating a linear relationship between $[B'_B]$ and δ. Good correlation for LSC46 at 900°C and 10^{-2}–1 atm was reported by the authors. It must be noted that this is a rather small interval of the high pO_2-range. Fits to our experimental data show that the $\{B'_B - V_O^{\bullet\bullet}\}^{\bullet}$ cluster model does not describe the oxygen non-stoichiometry of LSC46 equally well over the oxygen partial pressure range 10^{-5}–1 atm. The fit parameter α (defined as the fraction of unassociated oxygen vacancies) is limiting this model to oxygen non-stoichiometries $\delta < \frac{x}{1+\alpha}$ in the low pO_2-region. Thus, extrapolations of the $\{B'_B - V_O^{\bullet\bullet}\}^{\bullet}$ cluster model predict a plateau in vicinity of $\delta \approx 0.35$ for LSC46 (see Fig. 3), which has not been observed in experimental investigations. Application of the $\{B'_B - V_O^{\bullet\bullet}\}^{\bullet}$ cluster model to our oxygen non-stoichiometry data of LSF46 does not yield reasonable results since fit parameter α approaches unity, i.e. the cluster model coincides with the simple point defect model neglecting n-type charge carriers.

Conclusions

Various defect chemical models were applied to experimental oxygen non-stoichiometry data of the highly acceptor-doped perovskite-type oxides $La_{0.4}Sr_{0.6}CoO_{3-\delta}$ and $La_{0.4}Sr_{0.6}FeO_{3-\delta}$. It was found essential to take into account the simultaneous occurrence of three oxidation states of the B-site ions (point defect model), respectively *p*- and *n*-type charge carriers (electronic charge carrier model). Whereas a simple point defect model (neglecting the concentration of B^{2+}-ions) can be applied as an approximation for experimental data of the ferrite LSF46 in the high pO_2-region, it does not yield reasonable results for the cobaltite LSC46. The electronic charge carrier model is in close agreement with experimental data of LSF46 and further yields a more reasonable prediction for oxygen non-stoichiometry in the lower pO_2-range than the point defect model. We conclude that selected defect cluster models reported in literature are based on approximations which are not consistent with our experimental data. Neglecting concentrations of *p*- or *n*-type charge carriers (B^{4+}- or B^{2+}- ions), their applicability is often restricted to specific pO_2-regions and/or systems with low defect concentrations.

Acknowledgment

The authors gratefully acknowledge financial support by the Austrian Science Fund (FWF) within the Special Research Program 'Electroactive Materials' (project F915).

References

1. J. Mizusaki, Y. Mima, S. Yamauchi, K. Fueki, and H. Tagawa, *J. Solid State Chem.*, **80**, 102 (1989).
2. J. Mizusaki, M. Yoshihiro, S. Yamauchi, and K. Fueki, *J. Solid State Chem.*, **58**, 257 (1985).
3. E. Bucher, W. Sitte, I. Rom, I. Papst, W. Grogger, and F. Hofer, *Solid State Ionics*, **152/153**, 417 (2002).
4. E. Bucher, A. Benisek, and W. Sitte, *Solid State Ionics*, **157**, 39 (2003).
5. M.H.R. Lankhorst, H.J.M. Bouwmeester, and H. Verweij, *J. Solid State Chem.*, **133**, 555 (1997).
6. M.H.R. Lankhorst and H.J.M. Bouwmeester, *J. Electrochem. Soc.*, **144**, 1268 (1997).
7. Z. Yang and Y.S. Lin, *Solid State Ionics*, **150**, 245 (2002).
8. M. Cherry, M.S. Islam, and C.R.A. Catlow, *J. Solid State Chem.*, **118**, 125 (1995).
9. M.S. Islam, *Solid State Ionics*, **154/155**, 75 (2002).
10. J.A.M. van Roosmalen and E.H.P. Cordfunke, *J. Solid State Chem.*, **93**, 212 (1991).
11. V.L. Kozhevnikov, I.A. Leonidov, M.V. Patrakeev, E.B. Mitberg, and K.R. Poeppelmeier, *J. Solid State Chem.*, **158**, 320 (2000).
12. S. Diethelm, A. Closset, J. Van Herle, and K. Nisancioglu, *Electrochemistry*, **68**(6), 444 (2000).
13. L.Ya. Gavrilova and V.A. Cherepanov, in *Proc. of the 6th Int. Symp. on Solid Oxide Fuel Cells*, edited by S.C. Singhal and M. Dokiya (The Electrochemical Society, Pennington, NJ, 1999), Vol. 99-19, p. 404.